Supplementary Data

Solution based freeze cast polymer derived ceramics and isothermal wicking - relationship between pore structure and imbibition

Daniel Schumacher[1†], Dawid Zimnik[2†], Michaela Wilhelm[1*], Michael Dreyer[2] and Kurosch Rezwan[1,3]

1 Advanced Ceramics, Faculty of Production Engineering, University of Bremen, Am Biologischen Garten 2, IW3, Germany
2 Department of Fluid Mechanics, Center of Applied Space Technology and Microgravity (ZARM), Faculty of Production Engineering, University of Bremen, Am Fallturm 2, 28359 Bremen, Germany
3 MAPEX—Centre for Materials and Processes, University of Bremen, Am Fallturm 1, 28359 Bremen, Germany

† Equal authorship
* Corresponding author. Tel.: +49 421 218 64944; E-mail address: mwilhelm@uni-bremen.de.

Table S1. List of symbols.

Symbol	Quantity, Unit
A	cross section area, m^2
b	parameter of eq. 17, $s\ m^{-2}$
c	parameter of eq. 17, m^{-1}
D	diameter of the sample, m
d_{50}	mean particle size of filler particles, m
g	gravitational acceleration, $m\ s^{-2}$
H	height of the sample, m
H_{Darcy}	height of samples for Darcy test, m
h	wicking height, m
$\dot{h}$	interstitial velocity, $m\ s^{-2}$
h_{eq}	equilibrium height, m
j	water flux through lateral surface, $kg\ s^{-1}\ m^{-2}$
K_{Darcy}	permeability obtained by Darcy test, m^2

$K_{Wicking}$	permeability obtained from a wicking experiment, m^2
m	mass, kg
m_{eq}	equilibrium mass, kg
m_{sat}	mass of the completely saturated sample, kg
$m_{w,\ Darcy}$	mass of permeated water in Darcy test, kg
R_{Darcy}	radius of samples for Darcy test, m
R_{merc}	mean pore window radius obtained by mercury intrusion, m
R_s	static radius, m
r	radial direction according to coordinate system in Fig. 1
T_M	melting point, °C
t_{Darcy}	measurement time in Darcy test, s
u_s	superficial velocity, m s^{-1}
$\dot{V}$	volumetric flow rate, m^3 s^{-1}
z	axial direction according to coordinate system in Fig. 1
ΔL	length, m
Δp_{Darcy}	pressure difference in Darcy test, Pa
θ	contact angle, °
μ	dynamic viscosity, Pa s
ρ	density, kg m^{-3}
σ	surface tension, N m^{-1}
ϕ	open porosity, 1

Derivation of the Lucas-Washburn equation for porous media

Permeability K is the ability of a porous material to allow fluids to pass through it. It is a property of the porous material and is commonly defined by the Darcy law [1]. Different methods are proposed to determine the permeability of a porous structure in literature. Thus, the permeability can be determined for example by constant head permeability measurements, or as a fitting parameter of the viscous dominated part of the wicking experiment [2, 3, 4]. Both methods base on the Darcy law, which is given by

$$\frac{\Delta p}{\Delta L} = -\frac{\mu}{K} u_s. \tag{1}$$

To facilitate an overview all symbols used in equations are listed in Table S1. The permeability describes how easily a liquid can flow through a porous medium. The permeability is the parameter of the structure, which is related to the porosity, as well as to the shape of the pores. The superficial velocity u_s can be expressed in terms of the mass of liquid per unit time per unit area

$$u_s = \frac{\Delta m}{\rho A \Delta t} \tag{2}$$

with the cross section area

$$A = \frac{\pi}{4} D^2 \tag{3}$$

and an expression for the length $\Delta L = h_s$, the permeability can be determined from a flow measurement using

$$K = \frac{\mu h_s}{\Delta p} \frac{m}{\rho \frac{\pi}{4} D^2 t}. \tag{4}$$

Another method would be to fit the permeability to the viscous dominated part of the wicking experiment. This approach is also based on the Darcy equation *(1)*. The superficial velocity is replaced by the interstitial velocity $\dot{h}$ within the porous structure, given by

$$u_s = \phi \dot{h} \tag{5}$$

Furthermore, the length in the Darcy equation is replaced by the height of the wicking process $\Delta L = h$, which results in the following notation of the Darcy law.

$$\frac{\Delta p}{h} = \frac{\mu}{K} \phi \dot{h} \tag{6}$$

The driving force for the capillary rise is the capillary pressure resulting from the curvature of the liquid-vapor interface. It is expressed by the Young-Laplace equation

$$\Delta p = \frac{2\sigma \cos\theta}{R_s} \tag{7}$$

Rearranging equation (6) and equation (7), one obtains the Lucas-Washburn equation for porous materials [5, 6]

$$\dot{h}h = \frac{2\sigma \cos\theta \, K}{\phi \mu R_s}. \tag{8}$$

After separation of variables and the subsequent integration with $h(t = 0) = 0$ leads to

$$\frac{h^2}{t} = \frac{4\sigma \cos\theta \, K}{\phi \mu Rs}. \tag{9}$$

Since the weight-measurement technique was used in this work, the height in equation (9) was converted into a mass equation using the following equation.

$$m = \phi \rho A h \tag{10}$$

with

$$A = \frac{\pi}{4} D^2. \tag{11}$$

It follows

$$\frac{m^2}{t} = \frac{4\sigma \cos\theta \rho_l^2 A^2 \phi}{\mu_l} \frac{K}{R_s}. \tag{12}$$

With knowledge of the parameters of the porous structure and liquid parameters, the permeability can be determined using this equation. For this, the knowledge of m^2/t is required, which can be determined from the wicking experiment.

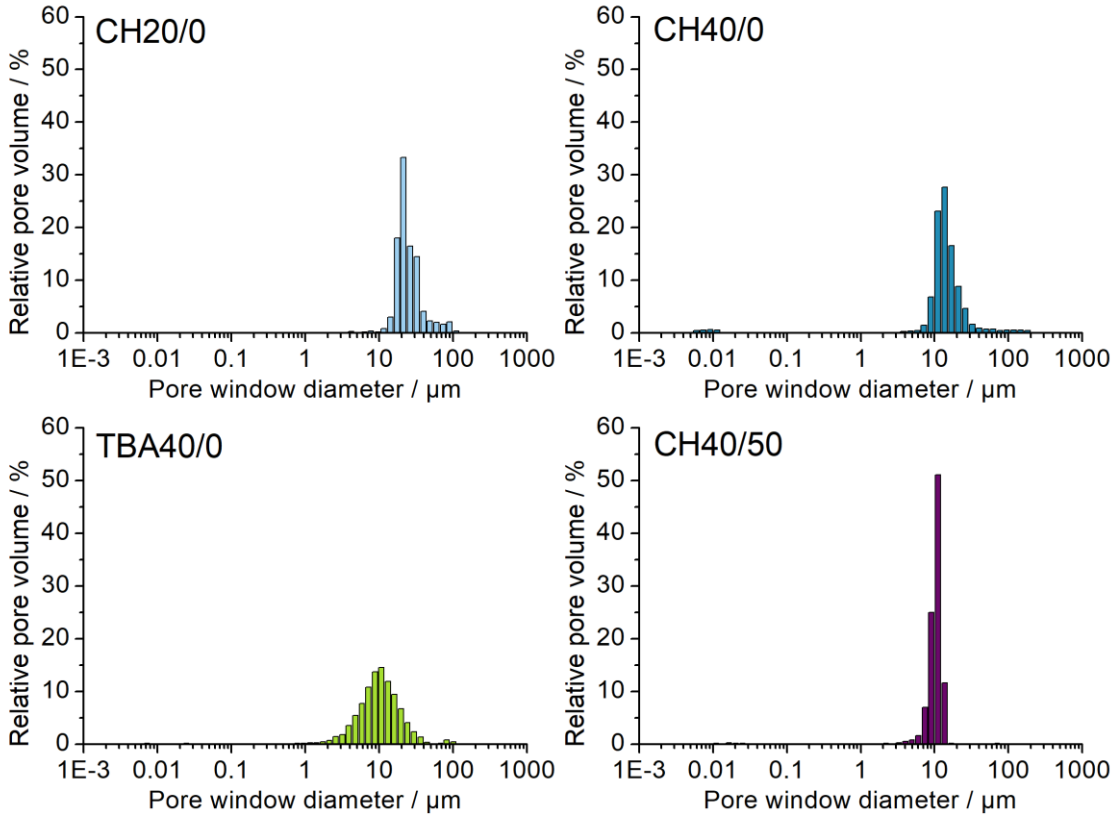

Figure S1. Relative pore volume obtained by mercury porosimetry for all investigated samples; exemplary only one measurement out of the three tests of each sample is shown.

Formation of lateral surface

In the past, a lot of research was conducted on suspension based freezing using different solvents as well as particles [7, 8, 9, 10]. Only few studies also investigated as part of the research the morphology of the lateral surface [11, 12]. They found porous lateral surfaces with slightly reduced permeability of a factor of 1.7 due to reduced pore sizes [11]. As demonstrated in Figure 5, the water flux *j(EC)* of the as prepared surface varies in dependence on the composition of the sample. But all samples show a larger ratio between open and closed surface as well as significantly lower water flux *j* in case of closed lateral surface compared to literature. Though a direct comparison with literature is not possible due to different pore morphology, pore size and porosity, it can be stated, that the lateral surface is significantly less permeable for samples presented in this work compared to previous studies.

Two main determining factors for the formation of a less permeable lateral surface should be described in the following. The first is the use of a silicon-coated PET film between mold and solution. Its very smooth and anti-adhesive surface prevents the formation of critical nuclei due to an absence of crystallization sites. Consequently, significantly less crystals are formed at the interface solution – film. The second factor is the difference in segregation mechanism between literature and this work. Previous research was conducted using suspended particles, hence suspension based freeze casting with the segregation process of particle rejection and entrapment between solvent crystals [11, 12]. In constrast, polymeric solutions which are used in this work segregate according to thermally induced phase separation [13, 14]. In suspension based freeze casting it can be assumed, that the particles can still be rejected and entrapped in between the crystals even though the crystals had approached already very close to the wall. Though the interaction of particles with the advancing solidification front is strongly influenced by parameters such as particle size, particle shape and freezing front velocity, this assumption is reasonable due to findings that the particles are for most cases displaced only by a fraction of their diameter in direction of freezing [15, 16]. This results in a very limited increase of particle concentration in front of the crystal tip and hence in the possibility that the crystal reaches the wall by rejecting all particles between the crystal tip and the wall. This is in correlation with previous studies showing open lateral surfaces for suspension based freeze casting [11]. In contrast to the segregation mechanism of particle rejection and entrapment, thermally induced phase separation results in an pronounced concentration profile with increased polymer concentration in front of the crystal tip [14]. Consequently, a dense solid layer is formed at the interface solution – wall. As a result, it can be stated that the prevention of nucleation on the interface solution – wall by a silicon-coated film and the segregation

mechanism of thermally induced phase separation are supposed to be main influential factors for the formation of a dense lateral surface

1. Darcy H. Les Fontaines Publiques de la ville de Dijon. Dalmont; 1856.
2. Fries N, Odic K, Conrath M, et al. The effect of evaporation on the wicking of liquids into a metallic weave. J Colloid Interface Sci. 2008;321(1):118-29. doi: 10.1016/j.jcis.2008.01.019.
3. Grebenyuk Y, Zhang HX, Wilhelm M, et al. Wicking into porous polymer-derived ceramic monoliths fabricated by freeze-casting. J Eur Ceram Soc. 2017;37(5):1993-2000. doi: 10.1016/j.jeurceramsoc.2016.11.049.
4. Siau JF. Transport processes in wood. Berlin: Springer; 1984.
5. Lucas R. Ueber das Zeitgesetz des kapillaren Aufstiegs von Fluessigkeiten. Kolloid Z. 1918;23:15-22.
6. Washburn EW. The Dynamics of Capillary Flow. Phys Rev. 1921;17(3):273-283.
7. Liu R, Xu T, Wang C. A review of fabrication strategies and applications of porous ceramics prepared by freeze-casting method. Ceram Int. 2016;42(2):2907-2925. doi: 10.1016/j.ceramint.2015.10.148.
8. Deville S. Ice-templating, freeze casting: Beyond materials processing. J Mater Res 2013;28(17):2202-2219. doi: 10.1557/jmr.2013.105.
9. Deville S. Freeze-Casting of Porous Biomaterials: Structure, Properties and Opportunities. Materials. 2010;3(3):1913-1927. doi: 10.3390/ma3031913.
10. Li WL, Lu K, Walz JY. Freeze casting of porous materials: review of critical factors in microstructure evolution. International Materials Reviews. 2013;57(1):37-60. doi: 10.1179/1743280411y.0000000011.
11. Seuba J, Leloup J, Richaud S, et al. Fabrication of ice-templated tubes by rotational freezing: Microstructure, strength, and permeability. J Eur Ceram Soc. 2017;37(6):2423-2429. doi: 10.1016/j.jeurceramsoc.2017.01.014.
12. Moon J-W, Hwang H-J, Awano M, et al. Preparation of NiO–YSZ tubular support with radially aligned pore channels. Materials Letters. 2003;57:1428 - 1434.
13. Naviroj M, Miller SM, Colombo P, et al. Directionally aligned macroporous SiOC via freeze casting of preceramic polymers. J Eur Ceram Soc. 2015;35(8):2225-2232. doi: 10.1016/j.jeurceramsoc.2015.02.013.
14. van de Witte P, Dijkstra PG, van den Berg JWA, et al. Phase separation porcesses in polymer solutions in relation to membrane formation. J Membr Sci. 1996;117:1 - 31.
15. Asthana R, Tewari SN. The engulfment of foreign particles by a freezing interface. J Mater Sci. 1993;28:5414 - 5425.
16. Rempel AW, Worster MG. The interaction between a particle and an adcancing solidification front. J Cryst Growth. 1999;205:427 - 440.